

Rapid Prototyping and Reverse Engineering Application for Orthopedic Surgery Planning

Dong-Gyu Ahn*

*Department of Mechanical Engineering, Chosun University,
375 Seosuk-dong, Dong-gu, Gwang-ju 501-759, Korea*

Jun-Young Lee

*Department of Orthopedics, Chosun University,
375 Seosuk-dong, Dong-gu, Gwang-ju 501-759, Korea*

Dong-Yol Yang

*Department of Mechanical Engineering, KAIST,
375-1 Science Town, Daejeon 305-701, Korea*

This paper describes rapid prototyping (RP) and reverse engineering (RE) application for orthopedic surgery planning to improve the efficiency and accuracy of the orthopedic surgery. Using the symmetrical characteristics of the human body, CAD data of undamaged bone of the injured area are generated from a mirror transformation of undamaged bone data for the uninjured area. The physical model before the injury is manufactured from Polyjet RP process. The surgical plan, including the selection of the proper implant, pre-forming of the implant and decision of fixation positions, etc., is determined by a physical simulation using the physical model. In order to examine the applicability and efficiency of the surgical planning technology, two case studies, such as a distal tibia comminuted fracture and an iliac wing fracture of pelvis, are carried out. From the results of the examination, it has been shown that the RP and RE can be applied to orthopedic surgical planning and can be an efficient surgical tool.

Key Words : Rapid Prototyping, Reverse Engineering, Physical Model, Orthopedic Surgical Planning, Bio-medical Engineering, Efficiency of Surgery

1. Introduction

Rapid prototyping (RP) technology has potential of a rapid manufacturing for three-dimensional parts with a geometrical complexity from a CAD model in the CAD/CAM environment (Kruth et al., 1998; Kulkarni et al., 2000). The application of RP technology has been extended to various fields such as engineering, manufac-

turing, medical science, education, industrial design and others (Yang et al., 2002; Wohler, 2004). Reverse engineering (RE) can directly generate CAD data from an actual object by measuring surfaces of the object through both contact and non-contact methods (Choi et al., 2001; Lee et al., 2001). In addition, the RE can easily evaluate the accuracy and the geometrical characteristics of the fabricated parts (Park et al., 2004). The combination of RP and RE has advantages of a rapid duplication for the real objects without the risk of damaging the object being duplicated (Petzold et al., 1997; Sun and Lal, 2002; Kim et al., 2004). Bio-medical engineering is one of the application areas that utilizes the advantages of the combination of RE and RP. Bio-medical applications of the RP technology now command

* Corresponding Author,

E-mail : smart@mail.chosun.ac.kr

TEL : +82-62-230-7043; **FAX :** +82-62-230-7234

Department of Mechanical Engineering, Chosun University, 375 Seosuk-dong, Dong-gu, Gwang-ju 501-759, Korea. (Manuscript Received January 25, 2005; Revised September 20, 2005)

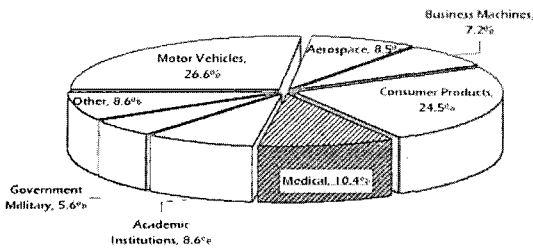


Fig. 1 Application area of rapid prototyping

10% of the market share for RP, as shown in Fig. 1 (Wohler, 2004).

Recently in the field of bio-medical engineering, new surgical technologies have been developed to improve the efficiency and the accuracy of surgery as well as to reduce inaccurate or incomplete surgical treatments. RAS (Robot-assisted surgery) and CAS (Computer-assisted surgery) are representative research areas related to these new surgical technologies (Kai et al., 1998). A surgical technology based on a combination of RP and RE using CT data has been introduced as an alternative of the CAS. One of the first researches on the combination of RP and RE using CT data for surgical planning was a cleft palate reconstruction in 1992 (Stoker et al., 1992; Webb, 2002). McGurk et al. (1997) used the SLA model for the planning of a maxillofacial surgery. Goto et al. (1997) manufactured three cases of the SLA model to predict an amount of bone needed to reconstruct jaw bones. Winder et al. (1997) fabricated a SLA model of a full skull, custom-made plate and the bone flap to assist manufacturing of custom-made titanium plate for a patient and to repair cranial defects.

Recently, the surgical technology utilizing the combination of RP and RE has been extended to applications in the area of orthopedic surgery. Potamianos et al. (1998) used SLA prototypes to visualize the fractured pelvis as well as to optimally fix an implant on the skull. Sanghera et al. (2002) preliminarily studied the feasibility of applying the combination of RP and RE to medical fields using FDM prototypes. In addition, they reported that use of a physical model for treatment planning and visualization instead of solely using software generated images can solve

problems, which is the difficulty in an accurate investigation of the complex anatomy among bone fragments in the vicinity of fracture sites, induced by viewing orientation uncertainties. Brown et al. (2002; 2003) reported the successful in-hospital application of RP models used in the surgical treatments for the case of the acetabular fractures, insertion pedicle screws into the spine, long-bone fractures, and joint fractures. They employed the reversed CAD data of the undamaged bone, which is the opposite data of the fractured region, and the Acquta 2100 and Z-CORP machines.

In this paper, the RP and RE application for orthopedic surgical planning is introduced to improve the efficiency and accuracy of the orthopedic surgery using symmetrical characteristics of the human body. The characteristics of the RP and RE application for orthopedic surgical planning are discussed. An error map is estimated to verify the dimensional accuracy of the physical shape of a bone. In order to investigate the feasibility of the application for the surgical planning, two case studies, such as a distal tibia comminuted fracture and an iliac wing fracture of pelvis, are carried out. In addition, the efficiency of the RP and RE application for orthopedic surgical planning is examined by comparing the results of surgery utilizing the surgical planning with those of the conventional surgery.

2. Rapid Prototyping and Reverse Engineering Application for Orthopedic Surgery Planning

The procedure of the RP and RE application for orthopedic surgical planning is illustrated in Fig. 2. The RP and RE application for orthopedic surgical planning utilizes the symmetrical characteristics of the human body. Computer Tomography (CT) simultaneously scans the injured and uninjured areas of a patient. The symmetry of the injured bone is verified by the scanned CT data. After the symmetry of the injured bone is confirmed, a surface reconstruction is performed using CT data of the uninjured bone. The first .stl data are subsequently generated from the recon-

structured surface. In case the target bone consists of a single piece, .stl data of both areas, which are the injured and uninjured area, are created, and the .stl data of the injured area is removed. The final CAD data of the original bone without damages in the injured area are generated from the mirror transformation of the intact bone data which is the opposite of the injured area.

Figure 3 shows the process flow to generate the .stl data of the original bone shape without the damage in the injured area. The optimal manufacturing data are generated by the CAD/CAM software of each rapid prototyping machine in four steps : determination of building direction, a slicing of the .stl data, generation of supports, and

an in-plane path generation. The physical model of the intact is manufactured from the RP apparatus in a layer-by-layer building process, as shown in Fig. 4. The pre-operative surgical planning is performed by a physical simulation using the physical model according to the following steps, as shown in Figs. 5 and 6 : (a) a selection of a proper implant, (b) a pre-forming of the implants, (c) a selection of fixation positions, (d) a decision of invasive sizes, (e) a decision of an approach route for the implants, and (e) a decision of an approach route of fixing devices for the implants. Finally, the surgical planning and the physical model are used to educate the operators.

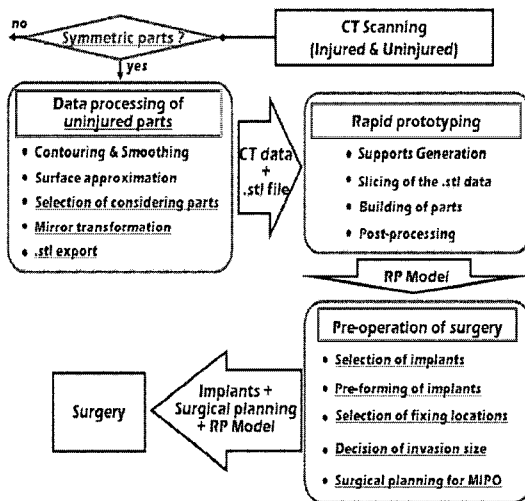


Fig. 2 Procedure of RP and RE application for orthopedic surgical planning

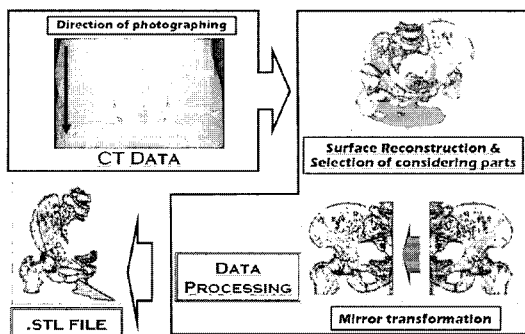


Fig. 3 Process flow to generate .stl data of the original bone shape for the injured area

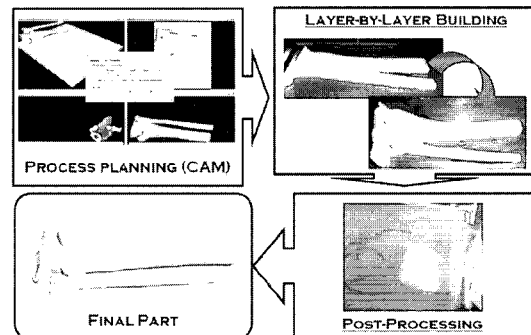


Fig. 4 Physical modeling procedure using original bone CAD data of injured area

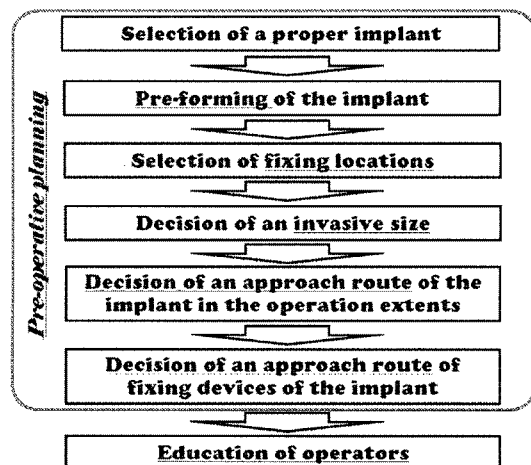


Fig. 5 Procedure of per-operative surgical planning using the physical model of the original bone shape for injured area

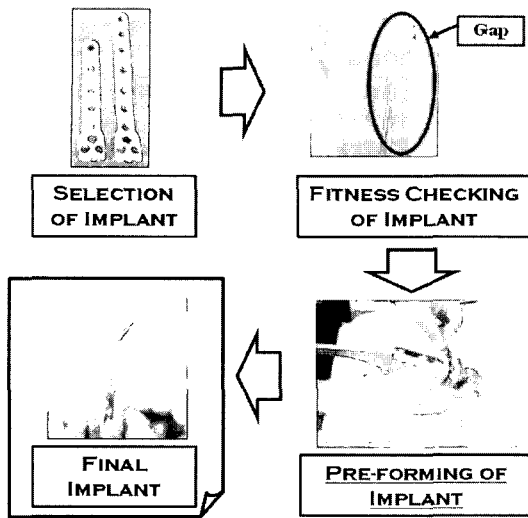


Fig. 6 Pre-operative surgical planning (Selection and pre-forming of implant)

3. Experiments

In order to investigate the applicability and the efficiency of RP and RE application for orthopedic surgical planning, two case studies, such as a distal tibia comminuted fracture and an iliac wing fracture of pelvis, are carried out.

CT data are generated by a Siemens Somatom Plus 4 scanner. Table 1 shows the slicing and feeding interval of the CT scanner. The CT data are stored in a DICOM format. The shape reconstruction of the CT data is performed by MIMICS 6.0 (www.materialise.com). The direction of the bone shape is identified by the CT data for each direction. Subsequently, the first .stl data are generated from the CT data. Editing of the first .stl data, deleting of the injured area and generation of a final CAD data through the mirror transformation of the undeleted data are carried out by Magic RP software (www.materialise.com).

The physical model is manufactured from the

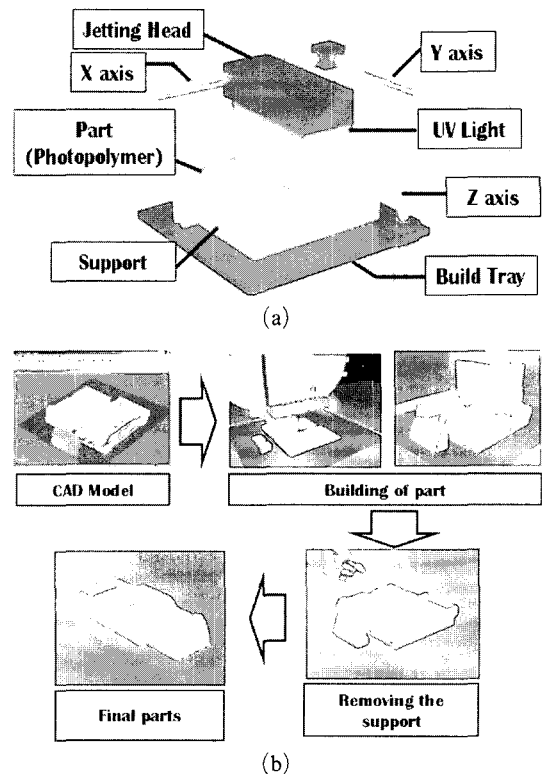


Fig. 7 Concept and building sequence of the Polyjet rapid prototyping process (www.sysopt.co.kr) : (a) Concept ; (b) Building sequence

Objet Quadra of Objet Geometries (www.2objet.com ; www.sysopt.co.kr). The Objet Quadra is the commercialized apparatus of Polyjet RP technology. In Polyjet technology, the jetting head with 1530 nozzles selectively shoots the photopolymer onto a previous layer in accordance with CAD data, and a UV beam subsequently cures the entire area with the shot photopolymer, as shown in Fig. 7. These processes are repeated until the final layer is completed. Through this process, a three-dimensional part is built rapidly. Because the layer thickness of the Polyjet technology is 0.02 mm, the fabricated prototype main-

Table 1 Slicing and feeding interval of CT scanner

Case	Slicing Interval (mm)	Feeding Interval (mm)
Distal tibia comminuted fracture	2.0	1.5
Proximal tibia plateau fracture	2.0	1.5
Iliac wing fracture of pelvis	3.0	2.0

tains a high dimensional accuracy. The previous research works have emphasized the importance of the selection for RP process to obtain an accurate physical model that is almost identical to the target bone shape (Webb, 2002). Hence, the Polyjet process, which is one of the highest precision RP processes, is selected as the proper RP process in this works.

In order to verify the dimensional accuracy of the physical model, an error map is estimated by comparing the final CAD data with the measured data of the physical model. A SNX-2W SG non-contact measurement system, which employs a white light and a halogen lamp as the lighting sources, and made use of a phase shift/gray code technique, is used to measure the physical model (www.solutionix.co.kr). The point cloud data of the entire shape for the physical model are obtained from a 360° measurement using a rotating table. The data manipulation, such as alignment, merging, decimation, etc, and estimation of the error map are performed by the EZ Scan software (www.solutionix.co.kr). The SNX-2W SG non-contact measurement system and EZ Scan software are developed by the Solutionix Inc.. The average error of the error map is automatically estimated by the EZ scan software.

Using the physical model, the surgical planning and education of operators are accomplished according to steps displayed in Fig. 5. The surgery is carried out by staff in the Department of Orthopedics of Chosun University Hospital. The results of surgery utilizing the surgical planning are compared with those of the conventional surgery of the department that did not utilize the surgical planning from the viewpoint of the surgical time, the number of X-ray exposures, the invasive size, and the patient's rehabilitation.

4. Results and Discussions

4.1 Distal tibia comminuted fracture

In the first case study, the patient had a fracture of the distal tibia in the left foot. The procedure from generation of CT data to the fabrication of the physical model is illustrated in Fig. 8. The symmetry of the injured and uninjured areas is

obvious, so that CT data of the distal tibia for the right foot are reconstructed by the MIMICS and MagicRP software. The original .stl data before the injury are created by the mirror transformation of the reconstructed data. The .stl data are generated within ten minutes. The volume of the .stl data is 71.9 (Width) × 92.5 (Length) × 200.1 (Height) mm³. In order to minimize the building time, the width is chosen to be the building direction. This is because the width is the shortest direction. The physical model is manufactured within approximately seven hours and fifty-eight minutes. The error map of the distal tibia shows that the average error is within 0.12 mm, as shown in Fig. 9. The results show that the physical model has a good geometrical conformity to the original .stl data. Table 2 shows the results of

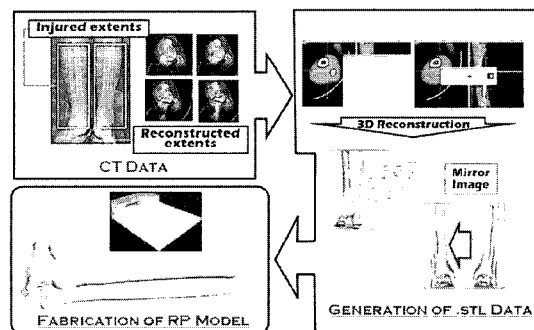


Fig. 8 Procedure of generation of CAD data and fabrication for physical model for the case of a distal tibia

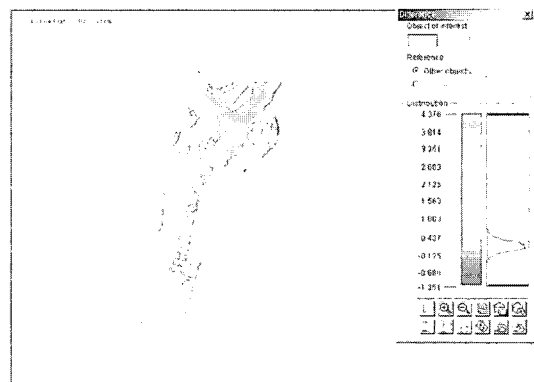


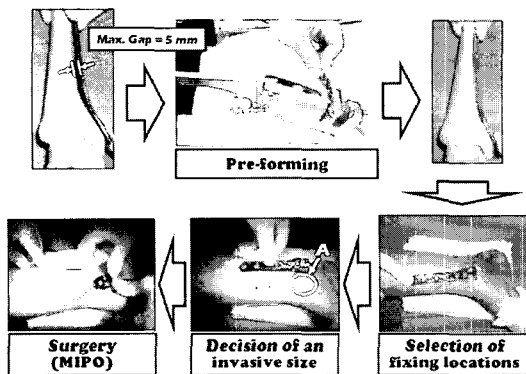
Fig. 9 Error map of the physical model for the case of a distal tibia

Table 2 Results of generation of CAD data and fabrication of physical model for the case of a distal tibia comminuted fracture

Generation time of .stl data (min)	Size of .stl data (MB)	Building interval (mm)	Building time (min)	Avg. error of the physical model (mm)
10	12	0.02	478	0.12

Table 3 Results of experiment for the case of a distal tibia comminuted fracture

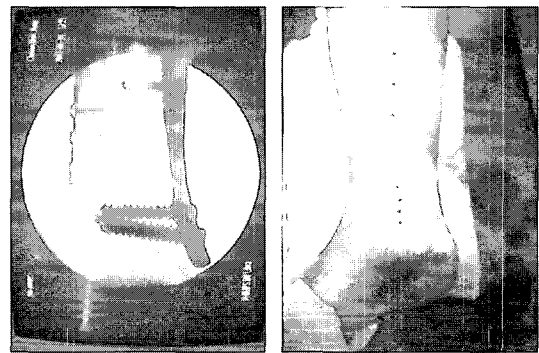
Surgical planning	Surgery time (min)	# of X-RAY exposures	Invasive size (cm)
The described surgical planning	≈40	1	3
Conventional planning	≈80-100	4	6

**Fig. 10** Procedure of pre-operative planning and operation of MIPO for the case of a distal tibia

generation for CAD data and the fabrication for physical model.

Figure 10 shows the procedure of the pre-operative surgical planning and the operation of a MIPO (Minimal Invasive Percutaneous Plate Osteosynthesis).

Using the physical model, a proper implant is chosen. In addition, the geometrical conformity of the implant to the contour of the bone model is verified. Although the implant is an anatomical plate reflected in statistical data of the human body, the results of comparing the shape of implant with that of the physical model show that the maximum difference between the selected implant and the physical model is 5 mm, as shown in Fig. 10. These results are due to the fact that the statistical data of the Korean physique are

**Fig. 11** Results of surgery for the case of a distal tibia

not reflected in the design data of the implant. Hence, the selected implant is preformed to obtain a good geometrical conformity of the implant to the contour of the physical model. The fixing locations of the implant are selected, as shown in Fig. 10. The incision area and the invasive size are selected as "A" in Fig. 10 and 3 cm, respectively. In addition, the penetration direction of the implant and the surgical procedure are confirmed.

Table 3 and Fig. 11 show the results of experiments for the case of the distal tibia comminuted fracture. The results of surgery show that the surgery time, the number of X-RAY exposures and the invasive size are approximately forty minutes, one time and 3 cm, respectively. Comparing the results of the surgery utilizing the described surgery planning with those of a conventional surgery performed by staff in the Ortho-

pedics Department of Chosun University Hospital, the surgery time, the number of X-RAY exposures and the invasive size are reduced by approximately fifty percent, seventy percent and fifty percent, respectively. The amount of radiation projected into the patient is decreased due to a reduction of number of X-RAY exposure needed to identify the position of the implant and the invasive size is reduced, so that it is ascribed that the morbidity of patients is highly reduced as well. MIPO has been available due to the reduction of the invasive size. The residual stress in the bone induced by a spring back of the implant and splitting between the bone and flesh are minimized due to the good geometrical conformity of the preformed implant to the fractured area of patient, so that the speed of the rehabilitation of the patient is remarkably enhanced.

4.2 Iliac wing fracture of pelvis

Tables 4 and 5 and Figs. 12~14 show the results of experiment for the case of the iliac wing fracture of a pelvis.

Because the pelvis is a single piece, the entire region of the pelvis is scanned by the CT apparatus. The first .stl data with the injured and uninjured area together are generated from the surface

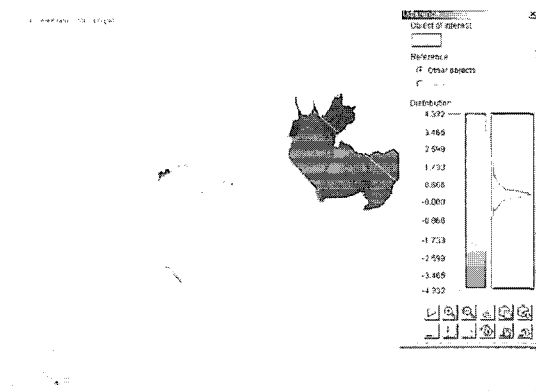


Fig. 12 Error map of the physical model for the case of a pelvis

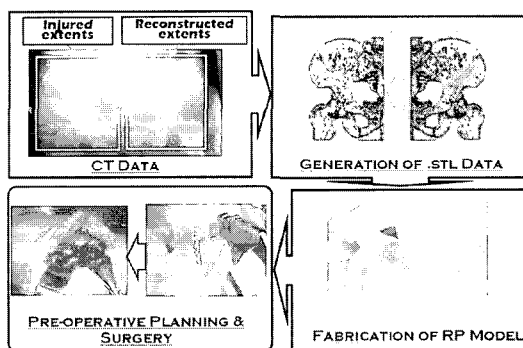


Fig. 13 Whole process for the case of an iliac wing fracture of pelvis

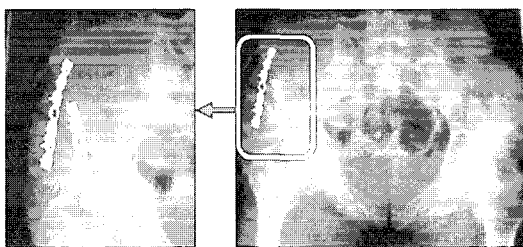


Fig. 14 Results of surgery for the case of an iliac wing fracture of pelvis

Table 4 Results of generation of CAD data and fabrication of physical model for the case of an iliac wing fracture of pelvis

Generation time of .stl data (min)	Size of .stl data (MB)	Building interval (mm)	Building time (min)	Avg. error of the physical model (mm)	Error of the region for wing (mm)
15	6.4	0.02	1,548	0.33	0.2

Table 5 Results of experiment for the case of an iliac wing fracture of pelvis

Surgical planning	Surgery time (min)	# of X-RAY exposures
The described surgical planning	≈45	2
Conventional planning	≈90-120	4

reconstruction of the CT data. The symmetry of the pelvis is obvious, therefore the second .stl data are obtained using only the uninjured area of the first .stl data. The final .stl data is created from the mirror transformation of the second .stl data. The final .stl data is generated within fifteen minutes. The volume of the final .stl data is $159.6 \times 246.2 \times 211.9 \text{ mm}^3$. Although a long building time is required, the building direction is selected as Y-direction to optimally support the model during the fabrication. The physical model without damages is manufactured within approximately twenty-five hours and forty-eight minutes. The error map shows that the average error maintains 0.33 mm, as shown in Fig. 12. The error of the region for wing is, however, less than 0.2 mm. Hence, it has been known that the physical model of the pelvis has a good geometrical conformity to the final .stl data in the region of wing.

Using the physical model, a proper implant is chosen, and the geometrical conformity of the implant to the uninjured bone shape is verified. Because the iliac wing of the pelvis has an excessive flexion on the surface of the bone shape, the selected implant needed to be able to easily bend in conformity with the bone shape. Hence, the pelvic reconstruction plate is chosen as the proper implant. Two pelvic reconstruction plates are needed to accurately fix the fractured area due to the geometrical characteristics of the iliac wing of the pelvis. The fixation locations of the implants, the position of the incision and the incision size are chosen using the preformed implants and the physical model. In addition, the establishment of the surgical planning and the education of the operators are carried out using the physical model and the preformed implants.

The results of the surgery show that the surgery time and number of X-RAY exposures are approximately forty-five minutes and two times, respectively. Comparing the results of the surgery utilizing the described surgery planning with those of a conventional surgery technology, the surgery time and the number of X-RAY exposures are reduced by approximately fifty percent each. The amount of radiation projected into the patient is decreased due to the reduction of num-

ber of X-RAY exposures needed to identify the position of the implant. The surgery is successfully carried out without a reworking of the implant, which is induced by the difference between the contour of the preformed implant and the bone shape of the patient, in the operating room. The residual stress in bone induced by a spring back of implant and splitting between bone and flesh are minimized due to a good geometrical conformity of the preformed implants to the fractured area of patient, so that the speed of the rehabilitation is remarkably enhanced.

In this case, the fabrication time of the physical model is longer than the time in the previous case. However, the surgery for the patient is scheduled to take place one week after the CT scan. Hence, the fabrication time of the physical model does not affect the surgery schedule. In addition, it has been found that the advantages of the physical modeling, such as the reduction of surgery time, the rapid rehabilitation and an accurate surgery, can overcome the disadvantages of the additional increasing in cost and time due to the fabrication of the physical model.

5. Conclusions

In this research, RP and RE have been applied to orthopedic surgical planning for fractured symmetrical bones to improve the efficiency of the orthopedic surgery.

The applicability and efficiency of the surgical planning technology have been demonstrated by two clinical case studies including a distal tibia comminuted fracture and an iliac wing fracture of pelvis. The results show that the establishment of a desirable surgical planning is possible in the pre-operative planning stage. From the results of the case studies, it has been shown that the surgical time, number of the X-RAY exposures and the invasive sizes are remarkably reduced due to a good geometrical conformity of the implants to the bone shape as well as the full understanding of geometrical characteristics of bones for the patient and the surgical planning of the operators. In addition, it has been found that the speed of a patient's rehabilitation is remarkably enhanced

due to the minimization of the residual stress in the bone induced by a spring back of the implant and a splitting between the bone and flesh. Based on the above results, it has been shown that the RE and RP can be applied to orthopedic surgical planning and can be an efficient surgical tool.

In the future, additional case studies, such as the complex bones with more serious damage, the bone deficiency with a congenital deformity and others, and an additional statistical evaluation in term of mechanical engineering and medical science should be performed to confirm the applicability and efficiency of the technology of surgical planning. In addition, the research on the selection of a proper RP process, which can overcome the disadvantages of high costs and a long building time to fabricate RP model, should be carried out.

Acknowledgments

This study was supported by research funds from Chosun University, 2004.

References

- Brown, G. A., Brenton, M. and Firoozbaksh, K., 2002, "Application of Computer-Generated Stereolithography and Interpositioning Template in Acetabular Fracture: A Report of Eight Case," *Journal of Orthopaedic Trauma*, Vol. 16, No. 5, pp. 347~352.
- Brown, G. A., Firoozabkhsh, K., Decoster, T. A., Reyna, J. R. and Moneim, M., 2003, "Rapid Prototyping: The Future of Trauma Surgery?," *The Journal of Bone and Joint Surgery*, Vol. 85-A, Supplement 4, pp. 49~55.
- Choi, H. R., Jun., Y., Chang, M., Rho, H. -M. and Park, S., 2001, "A Reverse Engineering System for Reproducing a 3D Human Bust," *Proceedings of KSPE Spring Annual Meeting 2001*, pp. 15~19.
- Goto, M., Katsuki, T., Noguchi, H. and Hino, N., 1997, "Surgical Simulation for Reconstruction of Mandibular Bone Defects using Photocurable Plastic Skull Models: Report of Three Cases," *Journal of Oral & Maxillofacial Surgery*, Vol. 55, pp. 772~780.
- Kai, C. C., Meng, C. S., Ching, L. S., Hoe, E. K. and Fah, L. K., 1998, "Rapid Prototyping Assisted Surgery Planning," *The International Journal of Advanced Manufacturing Technology*, Vol. 14, pp. 624~630.
- Kim, S. K. and Son, Y. R., 2004, "Investigation on Airflows in Abnormal Nasal Cavity with Adenoid Vegetation by Particle Image Velocimetry," *KSME International Journal*, Vol. 18, No. 10, pp. 1799~1808.
- Kruth, J. P., Leu, M. C. and Nakagawa, T., 1998, "Progress in Additive Manufacturing and Rapid Prototyping," *Annals of the CIRP*, Vol. 47, No. 2, pp. 525~540.
- Kulkarni, P., Marson, D. and Dutta, D., 2000, "A Review of Process Planning Techniques in Layered Manufacturing," *Rapid Prototyping Journal*, Vol. 6, No. 1, pp. 18~35.
- Lee, H. K., Kim, H. C. and Yang, G. E., 2001, "A Study on Digital Process of Injection Mold in Reverse Engineering," *Journal of the Korean Society of Precision Engineering*, Vol. 19, No. 6, pp. 160~165.
- McGurk, M., Potamianos, P., Aimis, A. A., Gooder, N. M., 1997, "Rapid Prototyping Techniques for Anatomical Modeling in Medicine," *Annals of the Royal College of Surgeons in England*, Vol. 79, pp. 169~174.
- Park, K. B., Kim, K. B., Son, K., Suh, J. T. and Moon, B. Y., 2004, "Construction and Measurement of Three-Dimensional Knee Joint Model of Koreans," *Transaction of the Korean Society of Mechanical Engineering*, Vol. 28, No. 11, pp. 1664~1671.
- Petzold, R., Zeilhofer, H. -F. and Kalender, W. A., 1997, "Rapid Prototyping Technology in Medicine — Basics and Applications," *Computerized Medical Imaging and Graphics*, Vol. 23, No. 5, pp. 277~284.
- Potamianos, P., Aims, A. A., Forester, A. J., McGurk, M. and Bircher, M., 1998, "Rapid Prototyping for orthopedic surgery," *Proceedings of the Institute Mechanical Engineering Part H: Journal of Engineering in Medicine*, Vol. 212, pp. 383~393.
- Sanghera, B., Naique, S., Papaharilaou, Y. and

Amis, A., 2001, "Preliminary Study of Rapid Prototypes Medical Models," *Rapid Prototyping Journal*, Vol. 7, No. 5, pp. 275~284.

Stocker, N. G., Mankovitch, N. J. and Valentino, D., 1992, "Stereolithographic Models for Surgical Planning: Preliminary Report," *Journal of Oral & Maxillofacial Surgery*, Vol. 50, pp. 446~471.

Sun, W. and Lal, P., 2002, "Recent Development on Computer Aided Tissues Engineering — a Review," *Computer Methods and Programs in Biomedicine*, Vol. 67, pp. 85~103.

Webb, P. A., 2000, "A Review of Rapid Prototyping (RP) Techniques in the Medical and Biomedical Sector," *Journal of Medical Engineering & Technology*, Vol. 24, No. 4, pp. 149~153.

Winder, J., Cooke, R. S., Gray, J., Fennin,

T. and Fegan, T., 1999, "Medical Rapid Prototyping and 3D CT in the Manufacture of Custom Made Cranial Titanium Plates," *Journal of Medical Engineering & Technology*, Vol. 23, No. 1, pp. 26~28.

Wohler, T. T., 2004, *Wholer's Report 2004, Rapid Prototyping & Tooling State of the Industry*, Wholer's Associates Inc.

Yang, D. Y., Ahn, D. G., Lee, C. H., Park, C. H. and Kim, T. J., 2002, "Integration of CAD/CAM/CAE/RP for Development of Metal forming," *Journal of Materials Processing Technology*, Vol. 125, pp. 26~34.

<http://www.materialise.com>

<http://www.solutionix.co.kr>

<http://www.sysopt.co.kr>

<http://www.2objet.com>